Assessment of gold nanoparticles as a size-dependent vaccine carrier for enhancing the antibody response against synthetic foot-and-mouth disease virus peptide

2010 Nanotechnology 21 195101

(http://iopscience.iop.org/0957-4484/21/19/195101)

Nanotechnology **21** (2010) 195101 (8pp) doi:10.1088/0957-4484/21/19/195101

Assessment of gold nanoparticles as a size-dependent vaccine carrier for enhancing the antibody response against synthetic foot-and-mouth disease virus peptide

Yu-Shiun Chen[1,5], Yao-Ching Hung[2,5], Wei-Hsu Lin[3] and Guewha Steven Huang[4]

[1] Department of Materials Science and Engineering, National Chiao Tung University, 1001 University Road, EE137, Hsinchu 300, Taiwan, Republic of China
[2] Department of Obstetrics and Gynecology, School of Medicine, China Medical University and Hospital, 91 Hsueh-Shih Road, Taichung 40402, Taiwan, Republic of China
[3] Institute of Nanotechnology, National Chiao Tung University, 1001 University Road, Hsinchu 300, Taiwan, Republic of China
[4] Department of Materials Science and Engineering, Institute of Nanotechnology, National Chiao Tung University, 1001 University Road, Hsinchu 300, Taiwan, Republic of China

E-mail: gstevehuang@mail.nctu.edu.tw

Received 22 December 2009, in final form 29 March 2010
Published 19 April 2010
Online at stacks.iop.org/Nano/21/195101

Abstract

To assess the ability of gold nanoparticles (GNPs) to act as a size-dependent carrier, a synthetic peptide resembling foot-and-mouth disease virus (FMDV) protein was conjugated to GNPs ranging from 2 to 50 nm in diameter (2, 5, 8, 12, 17, 37, and 50 nm). An extra cysteine was added to the C-terminus of the FMDV peptide (pFMDV) to ensure maximal conjugation to the GNPs, which have a high affinity for sulfhydryl groups. The resultant pFMDV–GNP conjugates were then injected into BALB/c mice. Immunization with pFMDV–keyhole limpet hemocyanin (pFMDV–KLH) conjugate was also performed as a control. Blood was obtained from the mice after 4, 6, 8, and 10 weeks and antibody titers against both pFMDV and the carriers were measured. For the pFMDV–GNP immunization, specific antibodies against the synthetic peptide were detected in the sera of mice injected with 2, 5, 8, 12, and 17 nm pFMDV–GNP conjugates. Maximal antibody binding was noted for GNPs of diameter 8–17 nm. The pFMDV–GNPs induced a three-fold increase in the antibody response compared to the response to pFMDV–KLH. However, sera from either immunized mouse group did not exhibit an antibody response to GNPs, while the sera from pFMDV–KLH-immunized mice presented high levels of binding activity against KLH. Additionally, the uptake of pFMDV–GNP in the spleen was examined by inductively coupled plasma mass spectroscopy (ICP-MS) and transmission electron microscopy (TEM). The quantity of GNPs that accumulated in the spleen correlated to the magnitude of the immune response induced by pFMDV–GNP. In conclusion, we demonstrated the size-dependent immunogenic properties of pFMDV–GNP conjugates. Furthermore, we established that GNPs ranging from 8 to 17 nm in diameter may be ideal for eliciting a focused antibody response against a synthetic pFMDV peptide.

(Some figures in this article are in colour only in the electronic version)

[5] These authors contributed equally to this work.

1. Introduction

Synthetic peptides have often been used in vaccines in recent years. However, carriers are also required to elicit a high antibody titer since the peptides are typically insufficiently immunogenic. To enhance the immune response, peptides may be coupled to carrier proteins, forming peptide–carrier constructs. Large proteins or toxoids, such as keyhole limpet hemocyanin (KLH) [1, 2], ovalbumin (OVA) [3, 4], bovine serum albumin (BSA) [5, 6], and tetanus toxoid (TT) [7, 8] are regularly used for such purposes. More specifically, this type of peptide vaccine technology has been implemented in immunization against influenza and other diseases [9–11].

Most carriers currently in use are not ideal. Some elicit strong antibody responses against themselves and suppress the immune response against the peptide. For biological compounds, only a few conjugation sites are available, leading to insufficient epitope presentation and the exposure of antigenic sites on the carriers themselves. Additionally, since many carrier proteins are not stable in solution, peptide–carrier conjugation may result in precipitates that render conjugation non-reproducible and complicate the analysis of end products. Thus, common vaccine carriers present several major drawbacks, indicating the need for improved carrier technology.

Before use as a vaccine carrier, basic parameters such as the toxicity, immunogenicity, and specificity of the substance need to be characterized. Gold nanoparticles (GNPs) have been previously utilized as carriers for drug delivery [12], cancer-cell imaging [13], and photo-activated therapeutics [14], as well as antigen carriers for antibody generation [15–18]. In particular, using 25 and 100 nm diameter pluronic-stabilized polypropylene sulfide (PPS) nanoparticles as vaccine carriers, it was demonstrated that humoral and cellular immunity in mice is dependent on antigen size and complement. After intradermal injection, 25 nm nanoparticles were efficiently transported into the lymphatic capillaries and draining lymph nodes, while 100 nm diameter nanoparticles were only 10% as efficient.

GNPs present many benefits as vaccine carriers. Their synthesis has been studied for decades and is based on a well-known reaction that is easy to perform in the laboratory. GNPs may be generated at a specific size, which is dictated by the reaction conditions. Furthermore, GNPs are stable in solution and cause a visually identifiable color change when they do aggregate. Additional benefits of GNPs include that gold is one of the most biocompatible materials currently known and has an unusually high affinity for sulfhydryl groups. This affinity allows tight conjugation to a peptide by adding an extra cysteine residue to the latter. However, as a general vaccine carrier, the *in vivo* toxicity, immunogenicity, specificity, and, most important of all, the size dependency of GNPs, are not clear at the present time.

Recent outbreaks of foot-and-mouth disease (FMD) have occurred in a number of countries, in particular in Taiwan in 1997 and the United Kingdom in 2001. This disease has debilitating effects on domestic cloven-hoofed animals, including weight loss, decreased milk production, and loss of draught power, resulting in reduced productivity for a considerable time [19]. These symptoms are caused by FMD virus (FMDV), a small, non-enveloped icosahedral virus with a single-stranded RNA genome of approximately 8400 nucleotides. An unusual structural feature of the outer capsid surface is the long and flexible loop of the VP1 protein [9, 20]. This loop, known as a G–H loop, forms a major antigenic site on the virus that includes at its apex an Arg–Gly–Asp (RGD) motif [21, 22]. The amino-acid sequence of this loop contains immunodominant T- and B-cell epitopes that can elicit a neutralizing antibody response; many studies have used the G–H loop in peptide vaccines.

The purpose of the current study was to investigate the potential use of GNPs as peptide vaccine carriers. GNP immunogenicity and specificity were evaluated using FMDV as the vaccine's peptide component and KLH as a control. In particular, since size plays a pivotal role in the endocytosis and toxicity of GNPs in cells [23–25] and in animals [26–28], we hypothesized that particle size may influence the efficacy of GNPs as vaccine carriers.

2. Materials and methods

Chemicals

$HAuCl_4$, sodium citrate, $NaBH_4$, HCl, HNO_3, H_2SO_4, H_2O_2, OsO_4, and other analytical grade chemicals were purchased from Sigma-Aldrich and Fisher Scientific.

Preparation and characterization of GNPs

GNPs with diameters of 2, 5, 8, 12, 17, 37, and 50 nm were synthesized as reported previously [29, 30]. The seed colloids were prepared by adding 1 ml of 0.25 mM $HAuCl_4$ to 90 ml of water and stirring for 1 min at 25 °C. Two milliliters of 38.8 mM sodium citrate were then added to the solution, followed by stirring for 1 min and the addition of 0.6 ml of freshly prepared 0.1 M $NaBH_4$ in 38.8 mM sodium citrate. The solution was stirred for an additional 5–10 min at 0–4 °C. Different GNP diameters, ranging from 2 to 50 nm, were generated by changing the volume of the seed colloid added. Reaction temperatures and times were adjusted to obtain GNPs of a larger size. All synthesized GNPs were characterized by ultraviolet (UV) light absorbance and their size was verified by electron microscopy and atomic force microscopy. To minimize the impact of unreacted chemicals on the experimental animals, the GNPs were further purified by precipitation at 10 000 rpm in a microcentrifuge, followed by dialysis against phosphate-buffered saline (PBS; pH 7.4) before injection into the animals.

Design of synthetic peptide

The sequence of pFMDV is (N-terminus) NGSSKYGDTSTNNVRGDLQVLAQKAERTL (C-terminus), representing amino-acid residues 131–159 of the VP1 protein of the FMDV O/Taiwan/97strain. The peptide sequence was synthesized with an added C-terminal cysteine residue using an ABI Peptide Synthesizer and Fmoc chemistry. The sequence of the

generated peptide was then verified by mass spectrometry and amino-acid composition analysis.

Preparation of pFMDV–carrier conjugates

KLH conjugates were synthesized as reported previously [9]. The cysteine-containing pFMDV was resuspended in distilled water at 1 mg ml^{-1} and the pH was adjusted to approximately 8.5 by the addition of dilute sodium hydroxide. Commercial maleimide-activated KLH (Pierce, Rockford, IL, USA) was reconstituted in 50 mM sodium phosphate, 0.15 M NaCl, and 0.1 M EDTA buffer (pH 7.2) at a final concentration of 10 mg ml^{-1}. The peptide and carrier were mixed at a 0.5 molar ratio of thiol to maleimide in 0.1 M sodium phosphate, 0.15 M NaCl, and 10 mM EDTA buffer (pH 7.2) and allowed to react at 25 °C, shielded from light. The conjugated complexes were purified by centrifugation and resuspended in PBS to a final concentration of 0.01 mg ml^{-1}. The conjugate was then separated from unreacted peptide and carrier by high performance liquid chromatography (HPLC).

The approach used to conjugate GNPs to peptide was based on titration methods [29]. An extra cysteine was added to the C-terminus of each peptide to improve binding to the surface of the GNPs. GNP–peptide conjugation was achieved by titrating the antigens into a GNP solution. This titration was monitored by UV absorption at the wavelength appropriate for each peptide to detect aggregation of unsaturated GNPs in the presence of 1 M NaCl. After reaching the saturation point, the conjugated complexes were purified by centrifugation and resuspended in PBS to a final concentration of 0.01 $\mu g\ \mu l^{-1}$.

Immunization of mice

Animal treatments were performed following the 'Guidelines for the Care and Use of Experimental Animals' issued by National Chiao Tung University (Hsinchu, Taiwan). Four-week-old male BALB/c mice were housed at 22 ± 2 °C in a 12 h light/dark cycle and fed standard rodent chow and water *ad libitum*. Mice were randomly assigned to experimental groups, with each group consisting of six mice.

Groups of 4-week-old BALB/c mice were administered intraperitoneal (IP) and subcutaneous (SC) immunizations containing (1) pFMDV–KLH conjugate or (2) pFMDV–GNP conjugates with diameters of 2, 5, 8, 12, 17, 37, or 50 nm. These antigens were administered in equal volumes of complete Freund's adjuvant. For all groups, the mice were immunized at weeks 0, 1, 2, 3, 5, 7, and 9 and blood was collected from the tail vein after 4, 6, 8, and 10 weeks. The sera were collected after centrifugation and stored at −20 °C. Animals were sacrificed at the end of the experiment by cardiac puncture under carbon dioxide anesthesia. The spleens were then isolated and the organ weights of all mice were measured.

Enzyme-linked immunosorbent assay (ELISA)

To coat a 96-well plate with GNP, each well was pretreated with 200 μl of 1 mM 3-aminopropyl-triethoxysilane (APTES) in ethanol at room temperature for 40 min. APTES encourages optimal crosslinking of GNPs to plastic wells, allowing an effective ELISA to be conducted [31]. The activated wells were washed with ethanol twice for 5 min, followed by distilled water for 5 min. GNPs (15 mM, 150 μl) were then added to the coated wells and incubated for 2 h at room temperature, followed by three distilled water washes and three washes with 0.5% Triton X-100 in PBS. To coat the wells with other antigens, 100 μl of antigen were added to the wells, followed by incubation at room temperature for 30 min and three PBS washes. Blocking of non-specific binding was performed by adding 100 μl of 3% BSA to the wells for 60 min at room temperature, followed by three PBS washes. Antibody binding was then conducted by adding 100 μl of diluted antiserum to the wells and incubating for 1 h at room temperature, followed by further washes with PBS. To develop the ELISA, horseradish peroxidase (HRP) conjugated anti-mouse immunoglobulin G (IgG), 2,2′-azino-di-(3 ethylbenzthiazoline sulfonic acid) (ABTS), and hydrogen peroxide were added to the wells sequentially, according to the manufacturer's instructions, and the antibody–antigen binding efficacy was monitored by measuring absorbance at 405 nm.

Gel electrophoresis

Samples were mixed with 1% Tris-buffered saline (TBS; Sigma-Aldrich) and loaded onto a 3% agarose gel (Sigma-Aldrich). Gel separation was then performed using an electrophoresis unit running at 80 V. Protein levels were then visualized by incubating the gels in Coomassie Brilliant Blue R-250 staining solution (Sigma-Aldrich), followed by washing in a destaining solution containing 70% methanol and 7% acetic acid.

Inductively coupled plasma mass spectrometry (ICP-MS)

For the total element determinations, standard solutions were prepared by diluting a multi-element standard (1000 mg l^{-1} in 1 M HNO_3) obtained from Merck (Darmstadt, Germany). Nitric acid (65%), hydrochloric acid (37%), perchloric acid (70%), and hydrogen peroxide (30%) of Suprapur® grade (Merck) were used to mineralize the spleen sections. These samples were then homogenized in 25 mM Tris and 12.5 mM HCl solution (pH 8) and centrifuged at 13 000 rpm for 1 h. The resultant supernatant was applied to the size-exclusion column of the HPLC system, which had been equilibrated with 25 mM Tris and 12.5 mM HCl buffer (containing 20 mM KCl), and eluted with the same buffer at a flow rate of 1 ml min^{-1}. The eluted fractions from the HPLC system were detected by ICP-MS (SCIEX ELAN 5000, Perkin Elmer) and the metal components were identified using a gold standard. The main operating conditions were as follows: RF power of 1900 W, carrier gas flow of 0.8 l min^{-1} Ar, and makeup gas flow of 0.19 l min^{-1} Ar. The isotope ^{197}Au was measured as an internal standard.

Transmission electron microscopy (TEM)

Small pieces of tissue were fixed in 2.5% glutaraldehyde in 0.05 M sodium cacodylate-buffered saline (pH 7.4) at room temperature for 2 h. This primary fixation was followed by

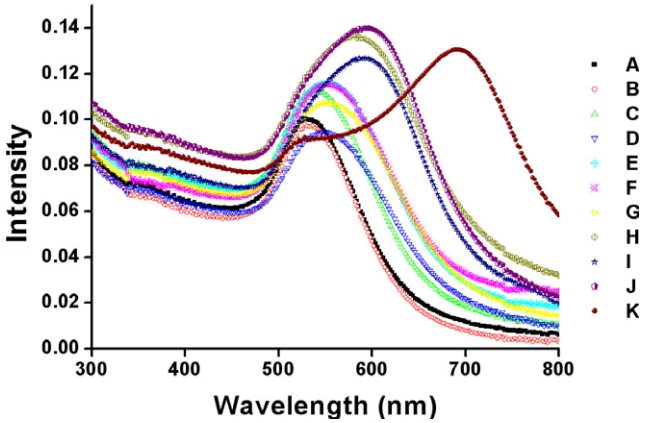

Figure 1. UV–vis absorbance measurements of GNPs. A shift of the surface plasmon band peaks correlated with different concentrations of peptides. Concentrations of pFMDV were: A, 1 μM; B, 0.9 μM; C, 0.8 μM; D, 0.7 μM; E, 06 μM; F, 0.5 μM; G, 0.4 μM; H, 0.3 μM; I, 0.2 μM; J, 0.1 μM; and K, 0 μM.

three 20 min washes with 0.05 M sodium cacodylate-buffered saline. The samples were then placed into 1% OsO_4 in sodium cacodylate-buffered saline at room temperature for 1 h. OsO_4 fixation was followed by three 20 min distilled water washes and dehydration in acetone. The samples were transferred successively to 33% and 66% Spurr resin/acetone solutions for 30 min each, followed by 100% Spurr resin for 5 h and fresh resin overnight.

Ultrathin 100 nm sections were produced using an ultramicrotome. The grids with ultrathin sections were post-stained with uranyl acetate for 30 min followed by lead for 3 min. After the post-staining procedure, a thin layer of carbon was evaporated onto the surface of the grids. The ultrathin sections were then examined using a Jeol 1400 and 3200 FS TEMs.

Statistical analyses

All data are presented as the mean ± SEM, with a minimum of six mice in each group. Concentrations of biogenic amines and Au in the spleen were analyzed using the unpaired Student's t-test. The criterion for statistical significance was $p < 0.05$ for all analyses.

3. Results

3.1. Preparation and analysis of pFMDV peptide and GNP conjugates

To further investigate the utility of GNPs as vaccine carriers, pFMDV was designed and synthesized based on its previously reported immunogenic epitope [9]. In particular, an extra cysteine residue was attached to the peptide's C-terminus to provide a sulfhydryl group as a conjugating site for the GNPs. The pFMDV was then conjugated to GNPs of various sizes (2, 5, 8, 12, 17, 37, and 50 nm in diameter). The synthesis of GNPs with varying diameters was monitored by UV absorbance (figure 1) and the resultant GNPs were examined by electron microscopy (figure 2). Conjugation of pFMDV–GNP was optimized by sodium chloride-induced aggregation [32]. More specifically, the lowest peptide concentration that did not cause a color change from red to dark blue, thus showing the lowest tendency to aggregate, was chosen for conjugation. The amount of pFMDV conjugated per GNP was also calculated as proportional to the surface area of the GNPs (figure 3). Conjugation of peptide to GNPs was analyzed by gel electrophoresis, which indicated that stable pFMDV–GNP conjugates were generated (figure 4).

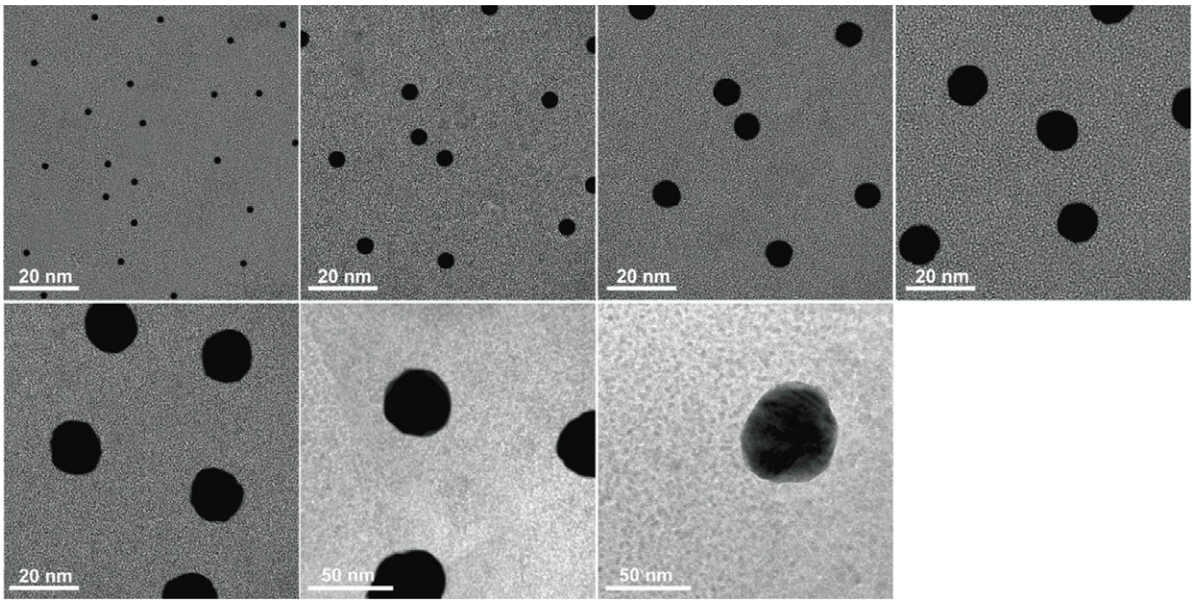

Figure 2. TEM images of synthesized GNPs. GNPs with diameters of 2, 5, 8, 12, 17, 37, and 50 nm were examined under an electron microscope. Scale bars are equal to 20 nm for images of 2, 5, 8, 12, and 17 nm GNPs, and equal to 50 nm for images of 37 and 50 nm GNPs.

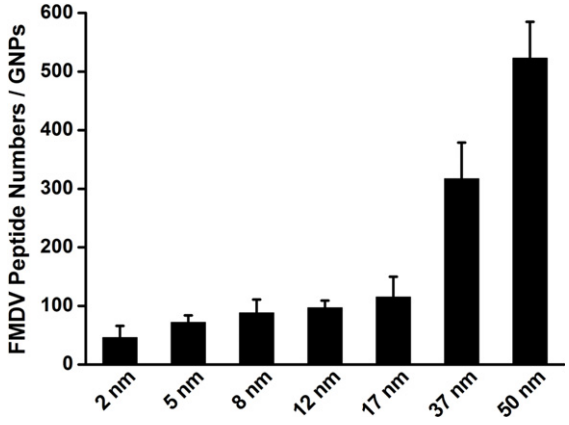

Figure 3. Number of pFMDVs conjugated to GNPs versus GNP diameter. The amount of conjugated pFMDV on the surface of the GNPs was calculated from the saturating concentration of the titration curves. The amount of conjugated pFMDV was proportional to the surface area of the GNPs.

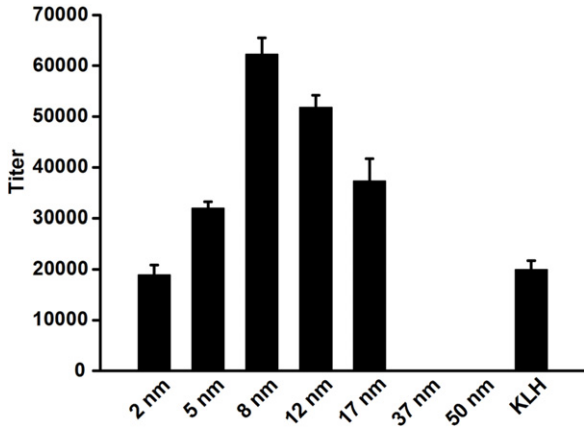

Figure 5. Titers of antisera withdrawn from pFMDV–GNP-injected mice on the sixth week of immunization. The values are averaged from samples derived from six different mice. The titer resulting from pFMDV–KLH immunization served as a control. Sera obtained from pFMDV–37 nm GNP- and pFMDV–50 nm GNP-injected mice did not exhibit detectable binding activity.

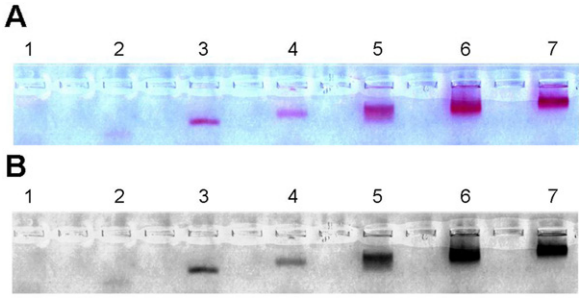

Figure 4. Gel electrophoresis of pFMDV–GNP conjugates. (A) Electrophoresis performed without staining. (B) Gel staining with Coomassie Brilliant Blue to indicate the presence of pFMDV. The difference in protein mobility was attributed to differences in the size of GNPs adsorbed to the pFMDVs. pFMDV–GNP conjugates were loaded as follows: lane 1, 2 nm GNPs; lane 2, 5 nm GNPs; lane 3, 8 nm GNPs; lane 4, 12 nm GNPs; lane 5, 17 nm GNPs; lane 6, 37 nm GNPs; and lane 7, 50 nm GNPs.

3.2. Induction of focused and enhanced antibody response by pFMDV–GNP conjugates

It has been shown that naked GNPs ranging from 8 to 17 nm in diameter are toxic to mice [26]. However, this toxicity is dose-dependent. In the current study, we administered GNPs at a dose of 0.5 mg kg^{-1}, which is one-sixteenth of the lethal dose and is apparently nontoxic to mice. Additionally, conjugation of pFMDV to the GNPs further reduced this *in vivo* toxicity, as the mice appeared healthy throughout the 10-week experimental period.

Mice were immunized with pFMDV–GNP conjugates that were prepared using GNPs of various sizes. Each injection contained equal amounts of pFMDV–GNP at a final concentration of 0.01 $\mu g\ \mu l^{-1}$. As a control, mice were injected with pFMDV–KLH at a final concentration of 0.01 mg ml^{-1}. These conjugates were injected IP and SC into BALB/c mice weekly, starting at week 0. Tail blood was collected after 4, 6, 8, and 10 weeks, followed by ELISA analysis to obtain titers of antisera against pFMDV, GNPs, and KLH (figures 5 and 6).

A significant antibody response was noted at week 6 (figure 5). The binding affinity of the antibodies, using pFMDV as the antigen, indicated size dependency. The pFMDV–2 nm GNP induced a titer of 19 000 ± 1900 at week 6, and this titer increased when GNP size was augmented. Antibody levels peaked when 8 nm diameter GNPs were administered (62 000 ± 3100) and then decreased to 0 for 37 and 50 nm GNPs at week 6. Meanwhile, the pFMDV–KLH conjugate exhibited a medium-strength antibody response, with a titer of 20 000 ± 1700. A three-fold enhancement of the antibody titers was observed using the GNPs as a carrier, as compared to using KLH.

When antibody responses at weeks 4, 6, 8, and 10 were integrated, a clear size-dependent relationship between GNPs and antibody levels was observed (figure 6(A)). GNPs ranging from 2 to 8 nm in diameter exhibited increasing binding affinity following subsequent immunizations, with the highest affinity associated with 8 nm GNPs. Meanwhile, a gradual decrease in the antibody titer was observed for the 12 and 17 nm diameter GNPs over time. We could not observe induced binding activity for the conjugates prepared with 37 and 50 nm diameter GNPs until the end of the experiment. In contrast to the GNP conjugates, the KLH conjugate exhibited medium-strength binding affinity.

The antibody response to carriers plays an important role in determining the immunogenicity of the conjugated peptide. While an ideal carrier should remain silent during immunization with peptide, KLH and other carriers are known to induce a significant immune response [2, 33, 34]. Antisera against KLH were observed beginning at week 4 and increased to a significant level (110 000 ± 6700) by week 10 (figure 6(B)). In contrast, GNPs, regardless of their size, showed no detectable antibody-binding activity over the course of our experiment. Thus, GNPs were demonstrated to be ideal candidate vaccine carriers due to their lack of immunogenicity.

In sum, we demonstrated that GNPs can act as vaccine carriers, inducing an approximately three-fold enhancement

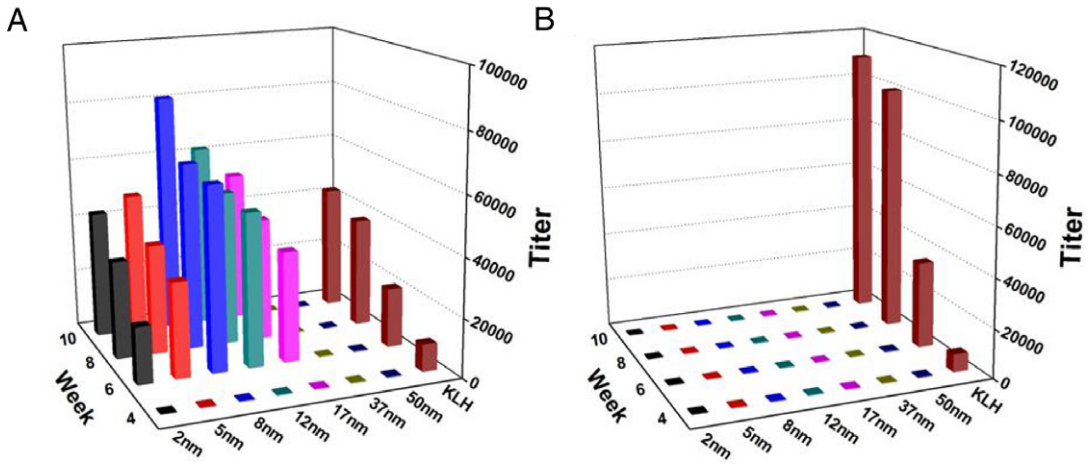

Figure 6. Titers of antisera from pFMDV–GNP-injected mice on weeks 4, 6, 8, and 10. The antigens used in the ELISA were (A) pFMDV and (B) GNPs/KLH. Titers of pFMDV–KLH were incorporated as a control.

in immunogenicity, as compared to responses elicited by the control vaccine carrier. Furthermore, the GNPs induced no detectable antibody binding when the two were incubated together. The GNPs used in this study thus possessed all of the positive characteristics of an ideal vaccine carrier.

3.3. Antibody response elicited by pFMDV–GNP conjugates associated with the number of GNPs taken up by spleen

The pFMDV–GNP conjugates may be taken up by antigen-presenting cells (APCs), including macrophages and dendritic cells. Typically, these APCs are transported by the circulation to the spleen. Epitopes presented on the surface of APCs are recognized by T cells, leading to subsequent T-cell activation. The presence and accumulation of pFMDV–GNPs in the spleen ensures the effective induction of an immune response toward the peptide.

The number of pFMDV–GNPs in the spleen was evaluated by ICP-MS (figure 7). The pFMDV–GNPs showed size-dependent biodistribution in the spleen. Indeed, their distribution profile in the spleen showed a striking similarity to their antibody-binding profile (figure 6), with maximal accumulation for the 12 nm GNPs.

The ability of GNPs to carry conjugated peptides into the spleen seemed to depend solely on the diameter of the GNP. When naked GNPs were injected into mice, their biodistribution in the spleen was almost identical to that of pFMDV–GNP conjugates (figure 7). This similarity indicated that surface modification of the GNPs did not alter their ability to enter the spleen. The similar biodistribution of naked and peptide-conjugated GNPs also demonstrated the size-dependent ability of GNPs to invade and accumulate in the spleen.

TEM was performed to verify the presence of GNPs in the spleen (figure 8) and showed that particles from 2 to 50 nm in diameter were trapped in splenic vesicles. The number of vesicular GNPs was minimal at diameters of 2 and 5 nm, maximal for diameters of 8 and 12 nm, and intermediate for 17–50 nm GNPs. These TEM results are consistent with the distribution profile obtained by ICP-MS.

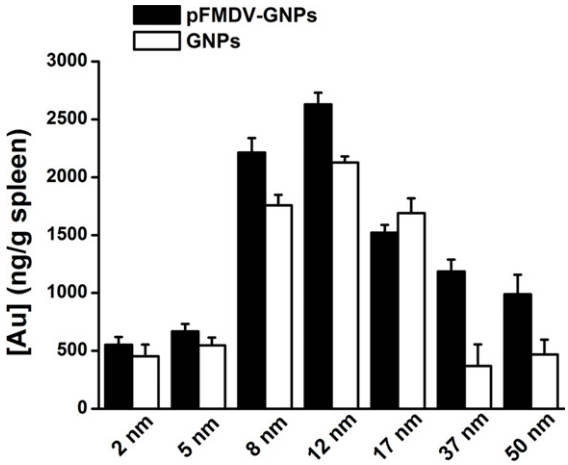

Figure 7. Distribution of GNPs in the mouse spleen. The pFMDV–GNP-injected mice were sacrificed at the end of the experiment. Numbers of GNPs in the spleen were then quantified by ICP-MS. Mice injected with pFMDV–GNPs are represented by the filled columns. The biodistribution of unmodified GNPs is represented by the empty columns. The values are averaged from six mice.

4. Discussion

A focused antibody response against haptens has several benefits. One application of such a strong response is more effective, less tedious production of monoclonal antibodies. This antiserum may also be used in assays that require highly specific antibody–antigen interactions, such as western blots. The benefits of the low response towards the gold particles are not only economic but also time-saving.

It was reported that peptide–KLH conjugates induce a strong immune response in mice. Additionally, KLH exhibits non-specific binding to the antigen and gives rise to false-positive binding due to this cross-reactivity. In this study, KLH induced a strong immune response against itself, with an antibody titer that was higher than that raised against pFMDV alone (figure 6). It is likely that conjugation of

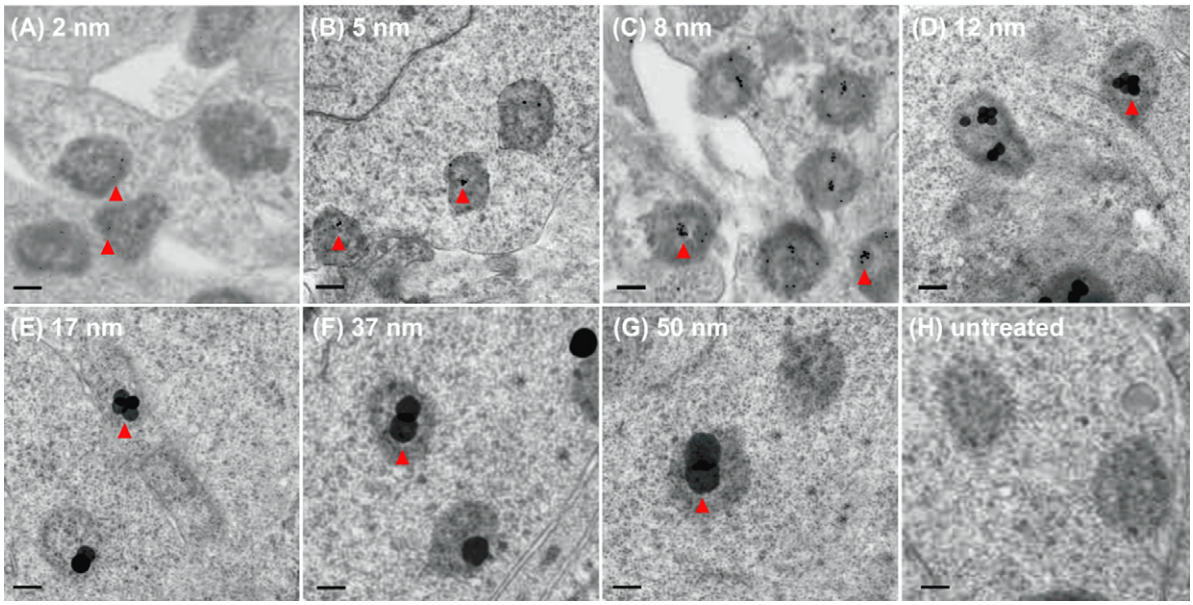

Figure 8. TEM images of spleens obtained from pFMDV–GNP-immunized mice. Mice were injected with pFMDV–GNPs of various GNP diameters: (A) 2 nm GNP, (B) 5 nm GNP, (C) 8 nm GNP, (D) 12 nm GNP, (E) 17 nm GNP, (F) 37 nm GNP, and (G) 50 nm GNP. The arrows indicate the aggregation and accumulation of GNPs in the vesicles of the spleen cells (scale bars are 20 nm).

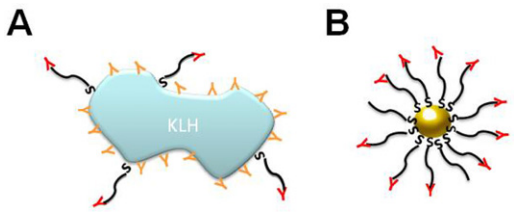

Figure 9. Schematic representation of the focused immunogenicity of KLH and GNPs as vaccine carriers. (A) Antibodies generated against peptide–KLH conjugates recognize epitopes displayed on both the peptide and KLH. (B) Antibodies generated by peptide–GNP conjugates selectively recognize peptide epitopes and rarely bind to the GNPs.

pFMDV to KLH generated potent antibody-recognition sites, thus complicating the induced antibody specificity. Antisera strongly recognized both the pFMDV–KLH conjugates and KLH alone, so specific binding to the synthetic pFMDV was seriously reduced (figure 9(A)).

In contrast to KLH carriers, the humoral response to GNPs is undetectable. However, when the GNPs were conjugated to pFMDV, they induced a strong antibody response specific to pFMDV, but rarely to the particles themselves (figure 9(B)). The finding indicates that the antibody response to synthetic pFMDV was not altered by conjugation to GNPs. GNPs are thus inert, rendering them ideal candidate vaccine carriers.

It is possible that the immune response induced by pFMDV is proportional to the number of peptides conjugated to the GNPs. However, this is unlikely because the total amount of peptide per injection remained constant. Furthermore, as determined by a titration test (figure 1) and gel electrophoresis (figure 4), the number of peptides per GNP was proportional to the particle's surface area (figure 3) but was not correlated with the size-dependent antibody response profile.

In rare cases, naked GNPs may induce antibody responses that affect the immunogenicity and specificity of peptide–GNP conjugates. In a previous study [35], we demonstrated that sera obtained from mice injected with GNPs that were 5 nm in diameter or smaller showed antibody-binding activity against the corresponding GNPs. However, the GNP-specific antibody titer was approximately 1000, which is at the lower boundary of titer values classified as positive binding. Adjuvant administration did not enhance the production of GNP-specific antisera, indicated by unchanged antibody binding to the GNPs. Therefore, the immunogenic binding activity of GNPs smaller than 5 nm in diameter is insignificant compared to the antibody response generated against the conjugated synthetic peptide.

The number of GNPs that accumulated in the spleen was size-dependent, as evaluated by ICP-MS (figure 7) and TEM (figure 8). The accumulation profile matched the size-dependent pattern of the immune response. This result is consistent with that of a previous nanovaccine study using 25 and 100 nm diameter pluronic-stabilized PPS nanoparticles as vaccine carriers [36]. This study demonstrated that generation of humoral and cellular immunity in mice is size- and complement-dependent. After intradermal injection, 25 nm nanoparticles were efficiently transported into the lymphatic capillaries and their draining lymph nodes, whereas 100 nm nanoparticles were only 10% as efficiently transported. Further studies should provide insights into the size-dependent immunogenicity of GNPs.

The potential benefits of using GNPs instead of traditional vaccine carriers are their low immunogenicity and ability to enhance the immune response to the conjugated peptide. Although this combination is seemingly contradictory, it may be realized by the size-dependent GNP biodistribution in the spleen, as observed by ICP-MS. It has been reported

that endocytosis is dependent on the size and shape of GNPs [23, 24]. In this study, GNP endocytosis reached a maximum when GNP diameter approached 50 nm. Additionally, larger GNPs tended to accumulate in the cells rather than in the circulation. It is possible that the majority of injected GNPs were absorbed at the site of injection [37] and that the slow release of larger particles resulted in a reduced number of larger particles in the blood. Consistent with this hypothesis, the majority of GNPs found in the circulation were 8–12 nm in diameter [27, 28]. Therefore, the accumulation of larger GNPs in the spleen could be due to size-dependent differences in GNP plasma concentration. The enhancement of the immune response by GNP carrier may thus be the consequence of increased localization to the spleen.

In the control group, unmodified GNPs also exhibited the same size-dependent biodistribution and the number of pFMDV–GNP conjugates in the spleen was higher than that of unmodified GNPs. These results indicate that peptide modification enhances both construct uptake by APCs and construct accumulation in the spleen.

Thus, we showed that the size-dependent immunogenicity of the pFMDV–GNP conjugates was associated with the number of GNPs taken up by the spleen. GNPs ranging from 8 to 17 nm in diameter may thus serve as ideal vaccine carriers, eliciting focused antibody responses against synthetic peptides.

5. Conclusion

In the current study, we evaluated the potential use of GNPs as vaccine carriers. GNPs possess several advantages over the traditional carrier KLH: pFMDV–GNPs induce a three-fold higher antibody response than pFMDV–KLH; GNPs alone do not induce an immune response; and the conjugation of peptide–GNPs is straightforward, mainly requiring additional incorporation of a cysteine residue into the C-terminus of the synthetic peptide. The optimal size range for the GNPs was 8–17 nm in diameter, as particles in this range stimulated the highest antibody levels and accumulated at the highest numbers in the spleen.

Acknowledgments

This study was supported in part by the National Science Council of Taiwan (grants NSC97-2923-B-009-001-MY3 and NSC 97-2320-B-009-002-MY3) and by the Bureau of Animal and Plant Health Inspection and Quarantine Council of Agriculture (grants 98AS-9.2.4-BQ-B1).

References

[1] Hou Y and Gu X X 2003 *J. Immunol.* **170** 4373–9
[2] May R J, Beenhouwer D O and Scharff M D 2003 *J. Immunol.* **171** 4905–12
[3] De Silva B S, Egodage K L and Wilson G S 1999 *Bioconjug. Chem.* **10** 496–501
[4] van Houten N E, Zwick M B, Menendez A and Scott J K 2006 *Vaccine* **24** 4188–200
[5] Rubinchik E and Chow A W 2000 *Vaccine* **18** 2312–20
[6] Riemer A B, Klinger M, Wagner S, Bernhaus A, Mazzucchelli L, Pehamberger H, Scheiner O, Zielinski C C and Jensen-Jarolim E 2004 *J. Immunol.* **173** 394–401
[7] Beenhouwer D O, May R J, Valadon P and Scharff M D 2002 *J. Immunol.* **169** 6992–9
[8] Maitta R W, Datta K, Lees A, Belouski S S and Pirofski L A 2004 *Infect. Immun.* **72** 196–208
[9] Shieh J J, Liang C M, Chen C Y, Lee F, Jong M H, Lai S S and Liang S M 2001 *Vaccine* **19** 4002–10
[10] Fan J *et al* 2004 *Vaccine* **22** 2993–3003
[11] Tompkins S M *et al* 2007 *Emerg. Infect. Diseases* **13** 426–35
[12] Paciotti G F, Myer L, Weinreich D, Goia D, Pavel N, McLaughlin R E and Tamarkin L 2004 *Drug. Deliv.* **11** 169–83
[13] Loo C, Lin A, Hirsch L, Lee M H, Barton J, Halas N, West J and Drezek R 2004 *Technol. Cancer Res. Treat.* **3** 33–40
[14] Pissuwan D, Valenzuela S M and Cortie M B 2006 *Trends Biotechnol.* **24** 62–7
[15] Tomii A and Masugi F 1991 *Jpn. J. Med. Sci. Biol.* **44** 75–80
[16] Dean H J, Fuller D and Osorio J E 2003 *Comp. Immunol. Microbiol. Infect. Dis.* **26** 373–88
[17] Dykman L A, Sumaroka M V, Staroverov S A, Zaitseva I S and Bogatyrev V A 2004 *Izv. Akad. Nauk. Ser. Biol.* **31** 86–91
[18] Vasilenko O A, Staroverov S A, Yermilov D N, Pristensky D V, Shchyogolev S Y and Dykman L A 2007 *Immunopharmacol. Immunotoxicol.* **29** 563–8
[19] Grubman M J and Baxt B 2004 *Clin. Microbiol. Rev.* **17** 465–93
[20] Carrillo C, Wigdorovitz A, Trono K, Dus Santos M J, Castanon S, Sadir A M, Ordas R, Escribano J M and Borca M V 2001 *Viral Immunol.* **14** 49–57
[21] Bittle J L, Houghten R A, Alexander H, Shinnick T M, Sutcliffe J G, Lerner R A, Rowlands D J and Brown F 1982 *Nature* **298** 30–3
[22] Strohmaier K, Franze R and Adam K H 1982 *J. Gen. Virol.* **59** 295–306
[23] Chithrani B D, Ghazani A A and Chan W C 2006 *Nano Lett.* **6** 662–8
[24] Chithrani B D and Chan W C 2007 *Nano Lett.* **7** 1542–50
[25] Hauck T S, Ghazani A A and Chan W C 2008 *Small* **4** 153–9
[26] Chen Y-S, Hung Y-C, Liau I and Huang G S 2009 *Nanoscale Res. Lett.* **4** 858
[27] Sonavane G, Tomoda K and Makino K 2008 *Colloids Surf.* B **66** 274–80
[28] De Jong W H, Hagens W I, Krystek P, Burger M C, Sips A J and Geertsma R E 2008 *Biomaterials* **29** 1912–9
[29] Brown K R, Walter D G and Natan M J 2000 *Chem. Mater.* **12** 306–13
[30] Liu F K, Ker C J, Chang Y C, Ko F H, Chu T C and Dai B T 2003 *Japan. J. Appl. Phys.* 1 **42** 4152
[31] Engvall E and Perlmann P 1971 *Immunochemistry* **8** 871–4
[32] Slot J W and Geuze H J 1985 *Eur. J. Cell Biol.* **38** 87–93
[33] Beekman N J, Schaaper W M, Turkstra J A and Meloen R H 1999 *Vaccine* **17** 2043–50
[34] Gharavi A E, Pierangeli S S, Colden-Stanfield M, Liu X W, Espinola R G and Harris E N 1999 *J. Immunol.* **163** 2922–7
[35] Chen Y S, Hung Y C, Liau I and Huang G S 2009 *Nanoscale Res. Lett.* **4** 858–64
[36] Reddy S T, van der Vlies A J, Simeoni E, Angeli V, Randolph G J, O'Neil C P, Lee L K, Swartz M A and Hubbell J A 2007 *Nat. Biotechnol.* **25** 1159–64
[37] Manolova V, Flace A, Bauer M, Schwarz K, Saudan P and Bachmann M F 2008 *Eur. J. Immunol.* **38** 1404–13